

Numerical prediction for airfoil Stall

Li Dong, Igor Men'shov, and Yoshiaki Nakamura (Nagoya University)

Abstract: Detached-Eddy Simulation is applied to three airfoils with different stall types. The method combines the Reynolds-averaged Navier-Stokes and Large Eddy Simulation approaches. Spalart-Allmaras approach^[1] is used, which reduces to the RANS formulation near a solid surface and to the subgrid model away from the wall. Results are compared with experiment data and RANS results. DES method shows an advantage with respect to RANS model in predicting stall angle and maximum lift for massive separated flow.

Key word: Detached-Eddy Simulation, Airfoil stall, Spalart-Allmaras turbulence model

Introduction

The present study concerns simulation of the flow field around an airfoil at a low speed and a large attack angle. The question is how accurately can stall characteristics be predicted by numerical simulation of highly separated flows.

RANS models can provide accurate results for attached boundary layer flows with minimal grid spacing requirement. However, they often fail in applications to large scale separated flows that depend on geometry. Large Eddy Simulation solve large, energy containing scales by modeling smaller scales. This method requires grid spacing to be prohibitively small. In boundary layers, energy containing eddies are so small that very small stream-wise grid spacing is needed.

Spalart et al.^[2] proposed Detached-Eddy Simulation (DES) approach that combines the most favorable elements of RANS models with Large Eddy Simulation. It can be applied to flows at high Reynolds numbers. In the present work, the DES method is used for three airfoils with different stall types.

Computational Approach

DES method is used in this paper for airfoil stall simulations. The pseudo time step is employed for both Navier-Stokes equations and Spalart-Allmaras turbulence equation. The LU-SGS method is used to implicitly discretize the S-A equation.

Governing Equation

The Navier-Stokes equations can be written in integral form as follows:

$$\frac{\partial}{\partial t} \iiint_{\Omega} \bar{w} d\Omega + \iint_{\partial\Omega} \bar{H} \cdot \bar{n} ds = \iint_{\partial\Omega} \bar{H}_V \cdot \bar{n} ds \quad (1)$$

where \bar{w} is the state vector of conservative

variables, \bar{H} and \bar{H}_V are inviscid and viscous fluxes, respectively. Being discretized with the finite volume method, the equation is then solved by using the dual time stepping method^[3] for unsteady simulation.

Spalart-Allmaras Model

The Spalart-Allmaras one equation model solves a partial differential equation for variable \tilde{u} which is related to turbulent viscosity.

$$\begin{aligned} \frac{D\tilde{u}}{Dt} = & c_{b1} [1 - f_{t2}] \tilde{S} \tilde{u} - \left[c_{w1} f_w - \frac{c_{b1}}{k^2} f_{t2} \right] \left[\frac{\mathbf{u}}{d} \right]^2 \\ & + \frac{1}{S} \left[\nabla \cdot ((\mathbf{u} + \tilde{\mathbf{u}}) \nabla \tilde{\mathbf{u}}) + c_{b2} (\nabla \tilde{\mathbf{u}})^2 \right] \\ & + f_{t1} \Delta U^2 \end{aligned} \quad (2)$$

where

$$\mathbf{u}_t = \tilde{u} f_{v1}, \quad f_{v1} = \frac{c^3}{c^3 + c_{v1}^3}, \quad c \equiv \frac{\tilde{u}}{u}$$

u is the molecular viscosity. The right hand side of Eq.1 composed of production, destruction, and diffusion terms.

Detached-Eddy Simulation

The DES formulation is based on a modification to the Spalart-Allmaras RANS model such that the model reduces to its RANS formulation near a solid surface and to a subgrid model away from the wall. It takes advantage of both RANS model in the thin shear layer and the power of LES to resolve geometry dependent and three dimensional eddies.

The DES formulation is obtained by replacing the distance to the nearest wall, d , by \tilde{d} , where \tilde{d} is defined as, $\tilde{d} \equiv \min(d, C_{DES} \Delta)$, where Δ is the largest one among the distances between a cell and its neighbors, and constant

$C_{DES} = 0.65$. Flow field was separated into two parts by length scale, as shown follow:

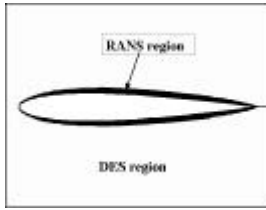


Fig.1 Division of flow-field

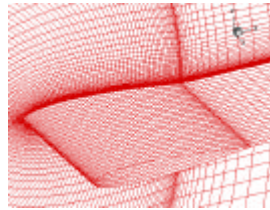


Fig.2 -D grid for airfoil

Results

The following three airfoils^[4] with different types of stall have been selected in this study.

1. NACA63₃-018 with trailing edge stall;
2. NACA63₁-012 with leading edge stall;
3. NACA64A-006 with thin airfoil stall.

The present calculation is performed for a Reynolds number of $5.8E10^6$ and a Mach number of 0.3. The grid used for 3-D flow field is shown in Fig.2

When the flow is separated, 3-D and unsteady, the effects of physical time step, inner iteration time step, and grid density are important. To make clear the character of flow field near stall, the third aerofoil NACA64A-006 is chosen for calculation.

Average lift

Free stream conditions in the non-dimension form are as follow:

$$V_{\infty} = 0.355$$

$$C = 1.0$$

$$T_{character} = C/V_{\infty} = 0.282$$

From Fig. 3, we can see that the average lift does not converge until $T > 10 \times T_{character}$. To obtain the convergence, we integrate the lift average it for increasing time periods. The results are shown in Fig.3:

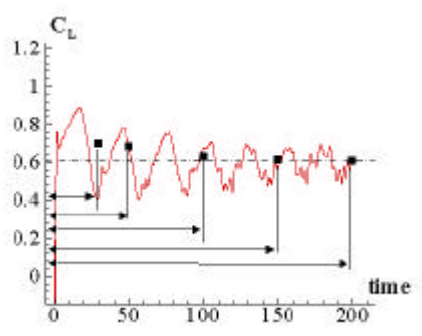


Fig.3 Average lift history

Time step accuracy

Two time steps, $\Delta t = 0.1$ (3.5% of the time the

free stream passes the chord length) and $\Delta t = 0.05$ (1.8%), are chosen to calculate the cases of 8° and 11° attack angles that are just before stall and after stall. As shown in Fig.4, the lift histories are almost same at for the attack angle 8° . For the angle 11° , lift histories are not same, but considering the average lift, drag and moment, no marked difference are observed.

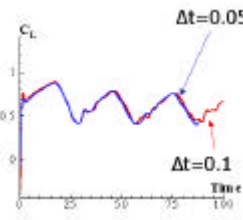


Fig.4 Lift history at AoA= 8°

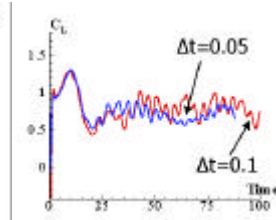


Fig.5 Lift history at AoA= 11°

Table 1

AoA= 8°	CL	CD	CM
EXP	0.76	0.098	-0.03
? t=0.1	0.604	0.085	-0.047
? t=0.05	0.606	0.086	-0.050
AoA= 11°			
EXP	0.81	0.18	-0.11
? t=0.1	0.763	0.162	-0.106
? t=0.05	0.783	0.169	-0.121

From this calculation we can see that, Δt near the value $\Delta t_c * C/V_{\infty}$ is appropriate for the unsteady simulation of airfoils, which is in line with the advice of Spalart,P.R.^[5]

Inner iterate steps

In present research work, an explicit local time stepping method is used for inner iterations. To show the effect of inner time steps, three different values are chose: 2, 20, 40. The lift histories are shown in Fig.6, the calculation starts from uniform flow field. Lift history are coincide with 20 and 40. Then 20 inner time steps are used in present work.

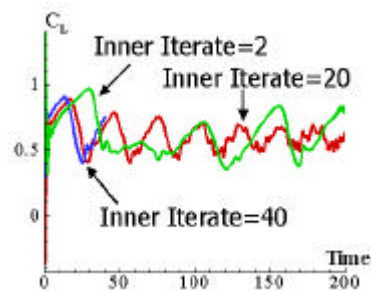


Fig.6 inner iterate steps effect

Grid density in Span

Since DES combines a property of LES, the grid density has an important effect. We increase the grid density along the span because the grid size directly affects separation between RANS region and LES region (we define the length scale as the smallest distance from the wall and the grid size, as stated above).

Two different grids are considered: $\Delta z=0.04$, and $\Delta z=0.02$. The lift history at $\text{AoA}=7^\circ$ and $\text{AoA}=8^\circ$ is shown in Fig. 7 and 8.

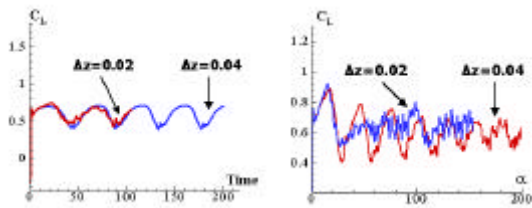


Fig.7 Lift history at $\text{AoA}=7^\circ$ Fig.8 Lift history at $\text{AoA}=8^\circ$

It should be noticed that at 7° , periodical behaviour is not changed, hence no average lift change appears. But for 8° degree the lift history is completely changed. As for the force in this case, we can see that the lift and drag are much more close to the experiment data, as can be seen in table 1.

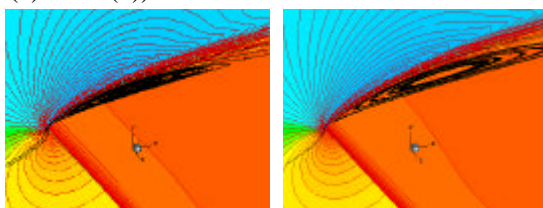
Table 2

$\text{AoA}=8^\circ$	CL	CD	CM
EXP	0.76	0.098	-0.03
$\Delta z=0.04$	0.604	0.085	-0.047
$\Delta z=0.02$	0.651	0.095	-0.070

Comparison with experimental data

The case of NACA64A-006

For this type of airfoil, as the attack angle increases, a separated bubble first appears on the upper surface near the leading edge. The lift increases almost linearly for small attack angles. The first non-linearity in the lift curve appears at $\alpha = 5.27^\circ$, as seen in Fig.12, which is due to a bubble produced near the leading edge (see Figs. 9(a) and 9(b)).



(a) $\alpha = 5.27^\circ$ (b) $\alpha = 6^\circ$

Fig.9 Flow field of NACA64A-006

The lift histories after bubble appear till stall occur, are shown as follow

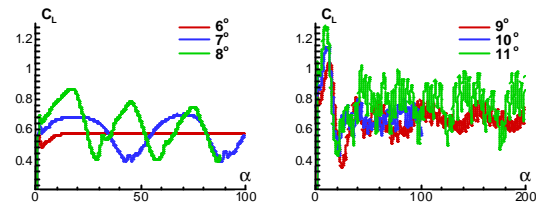


Fig.10 lift history from $\text{AoA}=7^\circ$ to $\text{AoA}=11^\circ$

Between 6° to 11° , there exist the case when the flow field appears clearly periodical phenomenon, at 6° degree, flow field is steady and 2D, at 7° degree, flow field become unsteady and period phenomena exist, this phenomena become disappear from 8° , and flow field show no disciplinarian after this attack angle.

Checking flow field at 7° degree at different time point found that large bubble over upper surface; small bubble follow with reattach and separation again; totally separated over upper surface are appeared periodically as time variety.

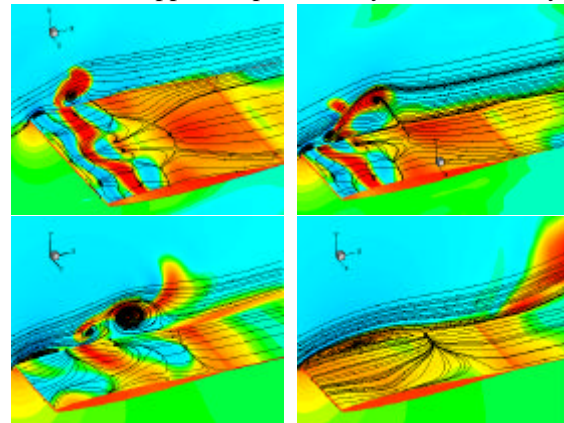


Fig.11 flow field at $\text{AoA}=8^\circ$

Lift curve are shown as follow, it is found that much more careful should be taken near the stall angle, especially just before the stall because of the bubble break down.

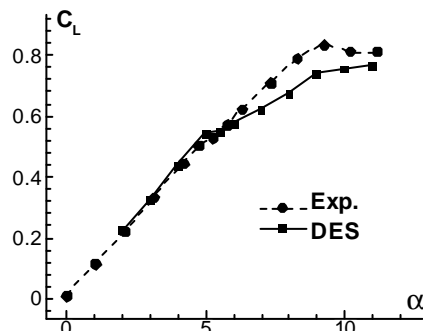
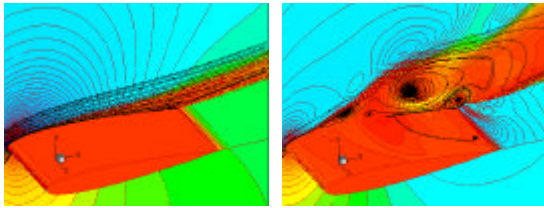


Fig.12 Lift vs. attack angle for NACA64A-006

The case of NACA63,-012

In this airfoil, as attack angle increases, the flow is suddenly separated from the leading edge, which covers all over the upper surface of airfoil, leading to lift loss after stall. The flow field is shown in Fig.13 (a) for before-stall case and Fig.13 (b) for after-stall case. By using RANS with B-L turbulence model, we can only catch the stall angle, but the lift after stall can't be simulated [4]. However, in the DES method, not only stall angle can be determined accurately, but also, large separated flow after stall can be simulated in detached region. The variation of lift with attack angle is shown in Fig.14.



(a) $\alpha = 14^\circ$ (b) $\alpha = 15^\circ$
Fig.13 Flow field of NACA63₁-012

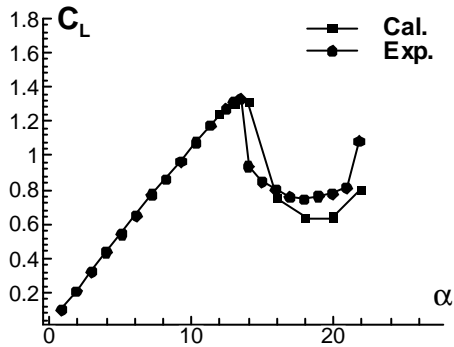
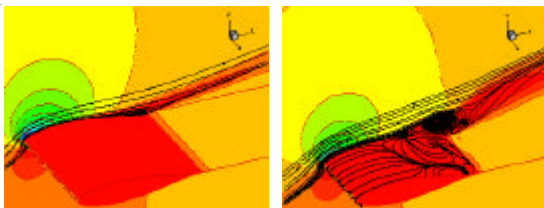


Fig.14 Lift vs. attack angle for NACA63₁-012

The case of NACA63₃-018

The lift loss in this case is caused by flow separation near the trailing edge, which extends rather slowly toward the upstream as attack angle increases. This process is shown in Figs.15 (a) and 15 (b). No obvious differences are observed between the RANS and DES methods, as shown in Fig.16. This means that, for slightly separated flows, use of the B-L turbulence model can provide reliable results.



(a) $\alpha = 15^\circ$ (b) $\alpha = 16^\circ$
Fig.15 Flow field of NACA63₃-018

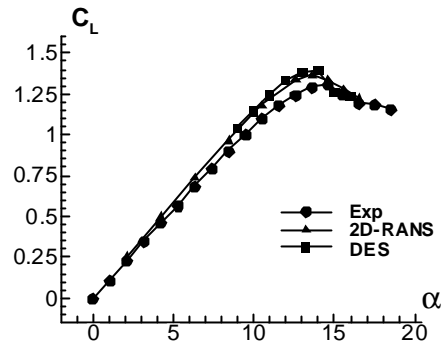


Fig.16 Flow field of NACA63₃-018

Conclusion

In this study, the properties of three different stall types of airfoil were simulated.

For the weakly separated flow fields, such as NACA63₃-018 at the attack angle just after maximum lift, DES gives good results for the lift. RANS method can also give the same result for the local upper surface separation.

For the massively separated flows, DES method shows much more reasonable results than RANS method.

Present calculations meet some difficulties in the case of a thin airfoil stall type, when the bubble become unstable and shows periodical variations. After full separation, present calculations again give reasonable results, as shown in the example NACA64A-006. In this case, span width, time step and other calculation conditions may affect the numerical result, and more research needs to understand these effects.

References

- [1] Spalart, P.R., and Allmaras, "A One-equation Turbulence model For Aerodynamic Flows" AIAA 92-0439.
- [2] Spalart, P.R., Jou, W.-H., Strelets, M., and Allmaras, S.R. Comments on the feasibility of LES for wings, and on a hybrid RANS/LES approach. 1st AFOESR Int. Conf. On DNS/LES, (1997), Ruston, LA. In Advances in DES/LES, C.Liu & Z.Liu Eds., Greyden Press, Columbus, OH.
- [3] Arnone, A., Liou, M.S., and Povinelli, L.A., "Integration of Navier-Stokes Equations Using Dual Time Stepping and a Multigrid Method" AIAA Journal, Vol.33, No.6, June 1995.
- [4] George, B. and Donald, E., "Examples of Three Representative Types of Airfoil

-
- Section Stall at Low Speed”, NACA TN-2502, 1951.
- [5] Spalart, P.R., Young-Person’s Guide to Detached-Eddy Simulation Grids, NASA/CR-2001-211032.
- [6] Morton, S., Forsythe, J.R., Mitchell, A., and Hajek, D., “Des and RANS Simulations of Delta Wing Vortical Flows”, AIAA 2002-0587.
- [7] Li Dong, Igor Men’shov, and Yoshiaki Nakamura, “2-D RANS Simulation for Three Different Stall Types”, Proceedings of the Thirty-fifth Fluid Dynamics Conference of Japan, Kyoto, Japan, 2003,9.
- [8] Baldwin, B.S. and Lomax, H., “Thin layer Approximation and Algebraic Model for Separated Turbulent Flows” AIAA 78-0238, 1978.
- [9] Squires, K.D., Forsythe, J.R., Morton, S.A., Strang, W.Z., Wurzler, K.E., Tomaro, R.F., Grismer, M.J., and Spalart, P.R., “progress on Detached-Eddy Simulation of Massively Separated Flows” AIAA 2002-1021.
- [10] Trong T.Bui, “Aparallel, Finite Volume Algorithm for Large-Eddy Simulation of Turbulent Flows” NASA TM-1999-206570.